



Matrix RGD ligand density and L1CAM-mediated Schwann cell interactions synergistically enhance neurite outgrowth



Nicole H. Romano^{a,1}, Christopher M. Madl^{b,1}, Sarah C. Heilshorn^{a,*}

^aMaterials Science and Engineering Department, Stanford University, Stanford, CA 94305, USA

^bBioengineering Department, Stanford University, Stanford, CA 94305, USA

ARTICLE INFO

Article history:

Received 27 May 2014

Received in revised form 1 October 2014

Accepted 4 October 2014

Available online 13 October 2014

Keywords:

Dorsal root ganglia

Nerve growth factor

Elastin-like peptide

L1CAM

RGD ligands

ABSTRACT

The innate biological response to peripheral nerve injury involves a complex interplay of multiple molecular cues to guide neurites across the injury gap. Many current strategies to stimulate regeneration take inspiration from this biological response. However, little is known about the balance of cell–matrix and Schwann cell–neurite dynamics required for regeneration of neural architectures. We present an engineered extracellular matrix (eECM) microenvironment with tailored cell–matrix and cell–cell interactions to study their individual and combined effects on neurite outgrowth. This eECM regulates cell–matrix interactions by presenting integrin-binding RGD (Arg–Gly–Asp) ligands at specified densities. Simultaneously, the addition or exclusion of nerve growth factor (NGF) is used to modulate L1CAM-mediated Schwann cell–neurite interactions. Individually, increasing the RGD ligand density from 0.16 to 3.2 mM resulted in increasing neurite lengths. In matrices presenting higher RGD ligand densities, neurite outgrowth was synergistically enhanced in the presence of soluble NGF. Analysis of Schwann cell migration and co-localization with neurites revealed that NGF enhanced cooperative outgrowth between the two cell types. Interestingly, neurites in NGF-supplemented conditions were unable to extend on the surrounding eECM without the assistance of Schwann cells. Blocking studies revealed that L1CAM is primarily responsible for these Schwann cell–neurite interactions. Without NGF supplementation, neurite outgrowth was unaffected by L1CAM blocking or the depletion of Schwann cells. These results underscore the synergistic interplay between cell–matrix and cell–cell interactions in enhancing neurite outgrowth for peripheral nerve regeneration.

© 2014 Acta Materialia Inc. Published by Elsevier Ltd. All rights reserved.

1. Introduction

Regeneration of the peripheral nervous system (PNS) after an acute injury requires a coordinated effort from macrophages, Schwann cells and neurons in order to achieve functional recovery [1,2]. After infiltrating macrophages have cleared debris from the injury site, Schwann cells from the distal nerve stump proliferate and migrate into the vacated endoneurial tubes [3]. These Schwann cells facilitate axonal regeneration both by direct Schwann cell–axon contact (through cell adhesion molecules such as L1CAM, NCAM and N-cadherin) and by synthesizing extracellular matrix components conducive to neurite extension (such as laminin and tenascin) [4,5]. Although significant advancements have been made in our understanding of post-injury regeneration in the PNS, the importance of relative interactions among Schwann cells,

neurons and the ECM remains unclear. We present the use of an engineered extracellular matrix (eECM) to strategically manipulate cell–matrix and Schwann cell–neuron contact to enhance neurite outgrowth from chick dorsal root ganglia (DRGs).

One of the greatest barriers to functional recovery in the PNS is the reconstruction of the highly organized neuronal–glial architecture [6,7]. In particular, the formation of a myelin sheath around axons depends critically on the ability of the ensheathing Schwann cell to polarize [8,9]. Intimate cellular contact on the adaxonal surface of the Schwann cell is maintained through cell adhesion molecules (CAMs) such as L1 cell adhesion molecule (L1CAM) and neural cell adhesion molecule (NCAM), as well as myelin-associated glycoprotein (MAG) [10,11]. On the other hand, the outer abaxonal surface of the Schwann cell binds to ECM proteins in the basal lamina [12–14]. This neural architecture presents an interesting division of labor between cell–matrix and cell–cell interactions [15]. First, we address the problem of regulating cell–matrix interactions by developing an eECM that presents cell–adhesive ligands at specified densities. Second, Schwann

* Corresponding author. Tel.: +1 650 723 3763; fax: +1 650 498 5596.

E-mail address: heilshorn@stanford.edu (S.C. Heilshorn).

¹ These authors contributed equally to this work.

cell–neuron interactions via L1CAM are enriched by stimulation with soluble nerve growth factor (NGF).

The integrin-binding RGD (Arg–Gly–Asp) sequence, native to a variety of ECM components, is widely studied due to its interaction with many of the classic integrin subunit combinations [16,17]. In its native contexts, the RGD sequence has been shown to stimulate Schwann cell migration and proliferation, as well as neurite extension in two- and three-dimensional systems [18–22]. Due to its ability to support neural outgrowth, the RGD peptide has also been incorporated in several eECM systems for neuronal culture [16,23–25]. For example, Schense and Hubbell [26] demonstrated that neurite outgrowth speed responds bimodally to the density of these integrin-binding RGD ligands when presented in the context of fibrin matrices; migration is inhibited at both very low and very high RGD ligand densities. The optimal ligand density for neurite outgrowth therefore requires sufficient integrin engagement to provide traction without inhibiting detachment from the substrate.

In order to isolate the effect of integrin-binding RGD ligands on neurite outgrowth, we previously incorporated a fibronectin-derived 17 amino acid sequence containing the RGD ligand into a protein-engineered material that does not otherwise mimic the amino acid sequence of native ECM components in the basal lamina [27]. This elastin-like protein (ELP) eECM confers mechanical resilience and elasticity appropriate for applications in neural regeneration, but exclusively limits receptor-specific binding to integrin–RGD partners [25]. Furthermore, by mixing two similar eECM components – one incorporating the bioactive RGD ligand and the other incorporating a non-binding RDG (Arg–Asp–Gly) sequence – we can control the density of integrin-binding sites presented on the hydrogel surface without altering the overall matrix density or mechanics of the eECM (Fig. 1A) [27].

NGF, a common supplement in the culture of DRG explants, is well known for its role in neurite outgrowth [25,28], chemotaxis [29] and neuron survival [30,31]. DRG sensory neurons express TrkA, a high-affinity receptor for NGF. In addition, NGF has low-affinity binding to p75 and the $\alpha_9\beta_1$ integrin (Fig. 1D). Binding of NGF to these low-affinity receptors is thought to result in the up-regulation of L1CAM in neurons [32]. In turn, L1CAM mediates signaling between neurons and Schwann cells, and is thought to play a role in successful PNS regeneration by mediating cell–cell communication [1,33–35]. Therefore, we hypothesized that withdrawing NGF supplementation from DRG cultures would result in altered neuron–Schwann cell interactions. Furthermore, there is some evidence that L1CAM engagement can potentiate integrin-mediated migration [36,37]. Together, these data prompted us to explore the potential interplay between cell–matrix and Schwann cell–neuron interactions within an engineered biomaterial context.

In this work, we show that the coordinated effect of L1CAM engagement and integrin–RGD binding synergistically enhances outgrowth of neurites from DRGs. The manipulation of cell–matrix and cell–cell interactions represents an important tool for coordinating and enhancing growth of neural tissues. Therefore, simultaneous stimulation of integrin-mediated adhesion and L1CAM engagement may be a useful strategy in the development of therapies for peripheral nerve regeneration.

2. Materials and methods

2.1. Preparation of elastin-like protein eECM

ELPs incorporating either cell-adhesive, fibronectin-derived extended RGD domains or inactive RDG domains were produced separately using recombinant protein engineering [27,38]. The full amino acid sequences for both proteins are shown in Fig. S1. Briefly, plasmids encoding the appropriate protein sequence for

ELPs were transformed into the BL21(DE3) strain of *Escherichia coli*. The bacteria were fermented in Terrific Broth medium to an optical density of 0.8, at which time 1 mM isopropyl β -D-1-thiogalactopyranoside was added to induce ELP production via the T7-lac promoter. After 4–6 h, the bacteria were pelleted and lysed by sonication in TEN buffer (0.1 M NaCl, 0.01 M Tris, 0.001 M EDTA at pH 8.0) with 1 mM phenylmethylsulfonyl fluoride protease inhibitor. Because ELPs exhibit lower critical solution temperature behavior, the desired protein could be purified from the cell pellet debris by repeated temperature cycling: at 4 °C, ELP was dissolved into H₂O and brought to pH 9.0; at 37 °C, ELP precipitation was aided by the addition of 1 M NaCl. The purified ELP was dialyzed against H₂O in a 10,000 molecular weight cutoff membrane to remove excess NaCl. The resulting protein product was verified by both sodium dodecyl sulfate–polyacrylamide gel electrophoresis and Western blot targeting of the His-tag at the N terminus. Sterilization of ELP was achieved by 0.22 μ m filtration and lyophilization.

2.2. ELP hydrogel formation

To fabricate 3 wt.% hydrogels, ELP in phosphate-buffered saline (PBS) at 3.75 wt.% was mixed with tetrakis(hydroxymethyl)phosphonium chloride (THPC) crosslinker in H₂O to a final concentration of 2.8 mM THPC, resulting in a stoichiometric ratio of one crosslinker functional group per primary amine on the protein backbone. In the case of hydrogels containing 3.2 mM RGD ligands, all ELPs in the precursor solution contained the cell-adhesive RGD domain. In order to achieve lower RGD ligand densities, the appropriate ratios of cell-adhesive and non-adhesive ELPs were mixed to 3.75 wt.% before adding crosslinker. The resulting precursor solution was pipetted into cylindrical silicone molds (5 mm diameter, 0.5 mm height) on glass coverslips and allowed to crosslink at room temperature for 10 min and at 37 °C for 30 min. The hydrogels were then submerged in the appropriate medium for 1 h at 37 °C before the addition of DRGs.

2.3. Isolation and culture of dorsal root ganglia

DRGs were isolated from E9 embryonic chicks and suspended in cold culture medium until placement on ELP hydrogels [39]. The culture medium consisted of Dulbecco's modified Eagle's medium with 10% fetal bovine serum (FBS) and 1% penicillin/streptomycin, with or without 50 ng ml⁻¹ nerve growth factor. For the Schwann cell-depleting treatment to select for a neuronal population, the medium also contained 7 μ M cytosine arabinoside. For L1CAM blocking studies, a 1:50 dilution of a monoclonal antibody directed against the L1-like antigen 8D9 was added to the culture medium. The 8D9 monoclonal antibody, developed by Dr. Vance Lemmon, was obtained from the Developmental Studies Hybridoma Bank, created by the NICHD of the NIH and maintained at the Department of Biology, University of Iowa. For conditioned medium experiments with Schwann cell-depleted cultures, DRG explants were treated with culture medium supplemented with 7 μ M cytosine arabinoside, in the presence or absence of 50 ng ml⁻¹ NGF. After 24 h, half of the culture medium was exchanged with conditioned medium obtained from 3 day cultures of intact DRG explants. After submerging ELP hydrogels in the appropriate medium, the isolated DRGs were carefully pipetted onto the surface of each hydrogel and incubated at 37 °C in 5% CO₂ and 100% humidity for 3 days without replenishing the medium.

2.4. Immunostaining of DRGs

After 3 days, the DRG cultures were immunostained for neurites (1:500, monoclonal mouse anti- β -III tubulin, Promega) and

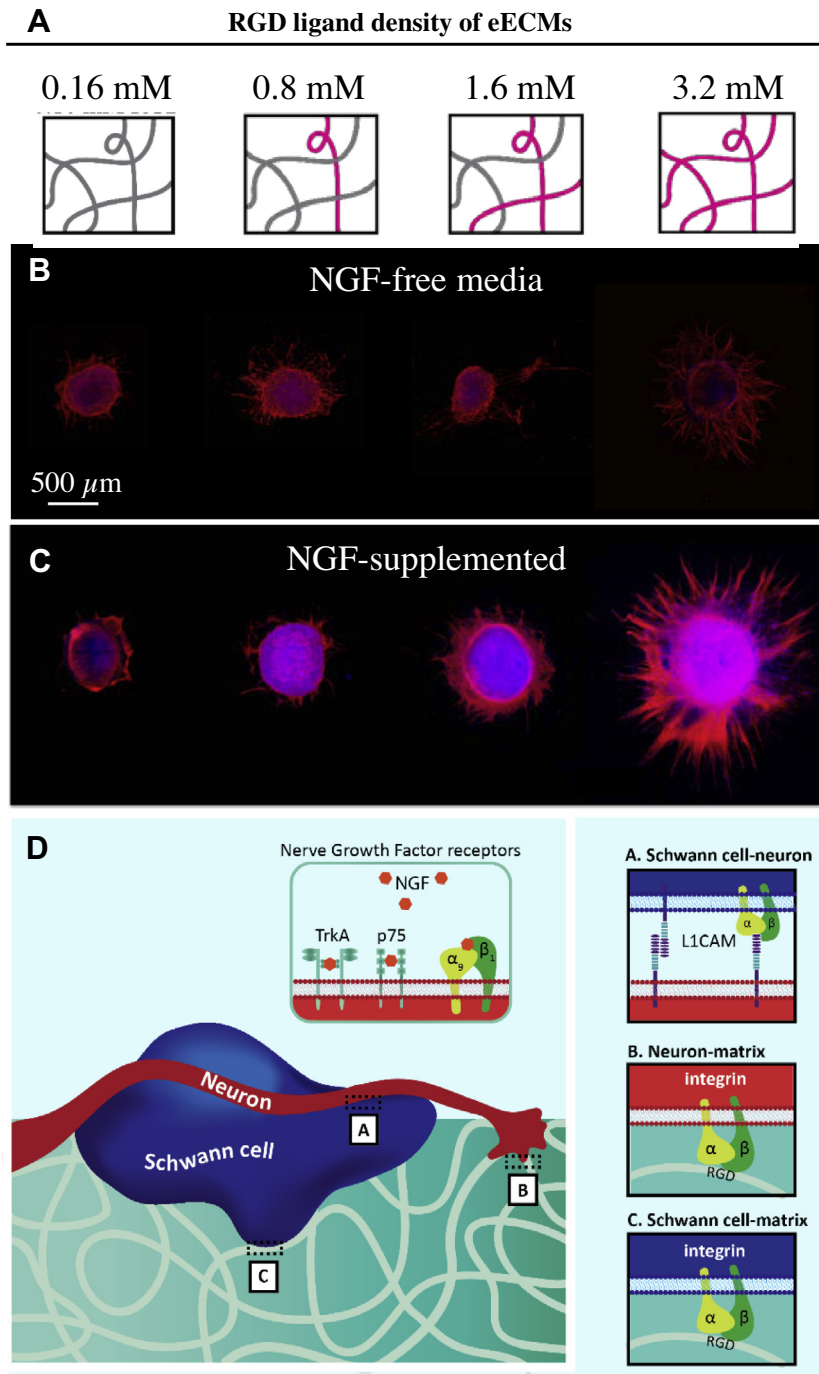


Fig. 1. Neurite outgrowth is synergistically enhanced by RGD ligand density and NGF supplementation. (A) Schematic of eECM with tunable RGD ligand density. (B and C) Representative images of neurite outgrowth on eECM with varying RGD ligand densities, without (B) and with (C) NGF supplementation in the culture medium. Red neurites (β -III tubulin) are overlaid on blue nuclei (DAPI). (D) Schematic of reported molecular mediators of cell-matrix and Schwann cell-neuron interactions.

Schwann cells (1:400, polyclonal rabbit anti-S100 protein, Sigma). At room temperature, the hydrogels were fixed in 4% paraformaldehyde for 1.5 h, washed three times in PBS and permeabilized using 0.25% Triton-X in PBS for 30 min. After blocking for 3 h in 5% bovine serum albumin (BSA) and 0.5% Triton-X in PBS, the hydrogels were incubated overnight in a solution of primary antibodies, 2.5% BSA and 0.25% Triton-X in PBS. The primary antibody solution was removed by rinsing repeatedly with PBS, and the hydrogels were incubated in a secondary antibody solution (goat anti-mouse AlexaFluor 546 at 1:500, goat anti-rabbit AlexaFluor

488 at 1:500, Life Technologies) overnight. Before imaging neurite outgrowth, samples were rinsed in PBS three times. Samples were mounted by carefully removing the silicone mold and inverting onto a droplet of ProLong Gold Antifade mounting solution (Life Technologies) on a coverslip. Using a Leica SPE confocal microscope, z-stacks 50–100 μm high (step size: 2.4 μm) were taken and tiled together in the x - y plane to visualize the entire DRG, as well as all surrounding neurites and migrating Schwann cells. For each channel, maximum projections of these tiled z-stacks were saved for downstream image analysis.

2.5. Imaging and data analysis

Neurite outgrowth was assessed using a modified version of a previously reported MATLAB script [25]. Briefly, maximum projections of the beta-III tubulin, S100 and DAPI stacks were input for each DRG. The script divided each DRG into 360 segments spanning 1° each and recorded the longest β-III tubulin-positive neurite in each segment (Fig. 2A). Neurite length was defined as the shortest distance between the neurite tip and the DRG explant boundary, as identified manually by the user. The same MATLAB script was used to evaluate the maximum migration of Schwann cells by identifying the DAPI-stained nuclei that appeared farthest from the edge of the DRG within each 1° segment (Fig. 2C). The difference between the Schwann cell migration front and the neurite outgrowth distance from the average Schwann cell migration front. Finally, co-localization of Schwann cells with neurites was evaluated using ImageJ. In the DAPI channel, the number of nuclei outside the DRG edge was determined using the Analyze Particles function. Next, a mask consisting of the beta-III tubulin channel was overlaid in order to obscure any nuclei co-localized with beta-III tubulin positive neurites. The Analyze Particles function was run again, revealing the proportion of cells migrating out of the DRG that were not co-localized with a neurite.

2.6. Regulation of cell adhesion molecules and integrin subunits

Three DRGs were manually pipetted onto each culture substrate, with 12 culture substrates per experimental condition. RNA was isolated using an RNAqueous-Micro Total RNA Isolation

kit (Ambion). The DRGs and ELP gel on which they were cultured were transferred to lysis buffer and mechanically disrupted by sonication. RNA was extracted following the manufacturer’s protocol and residual genomic DNA was removed by treating with DNase. A 100 ng aliquot of RNA per sample was reverse transcribed using a High-Capacity cDNA Reverse Transcription Kit (Applied Biosystems). Quantitative reverse transcription polymerase chain reaction (RT-PCR) was performed using Fast SYBR Green Master Mix (Applied Biosystems) on an Applied Biosystems StepOnePlus Real Time PCR System. The primers used for RT-PCR are listed in Table S1. GAPDH was used as an endogenous control.

2.7. Statistical analysis

Neurite outgrowth and Schwann cell migration were quantified for 6–13 DRGs for each of the eight conditions (0.16 mM RGD, 0.8 mM RGD, 1.6 mM RGD and 3.2 mM RGD, each with and without 50 mg ml⁻¹ NGF), in order to ensure that at least 1000 neurites and Schwann cells were analyzed for each condition. Because neurites extending from the same DRG were found to exhibit highly correlated lengths, a sub-sampling method was used to account for within-sample correlations [40,41]. This method used a simple average-of-averages approach with propagation of a standard error to account for the existence of pseudo-replicates. Two-way analyses of variance (ANOVAs) provided significance values for the effect of three parameters on neurite outgrowth and Schwann cell migration: RGD ligand density, NGF supplementation and an interaction term. For post-hoc *t*-tests, a Bonferroni correction was applied to account for multiple comparisons.

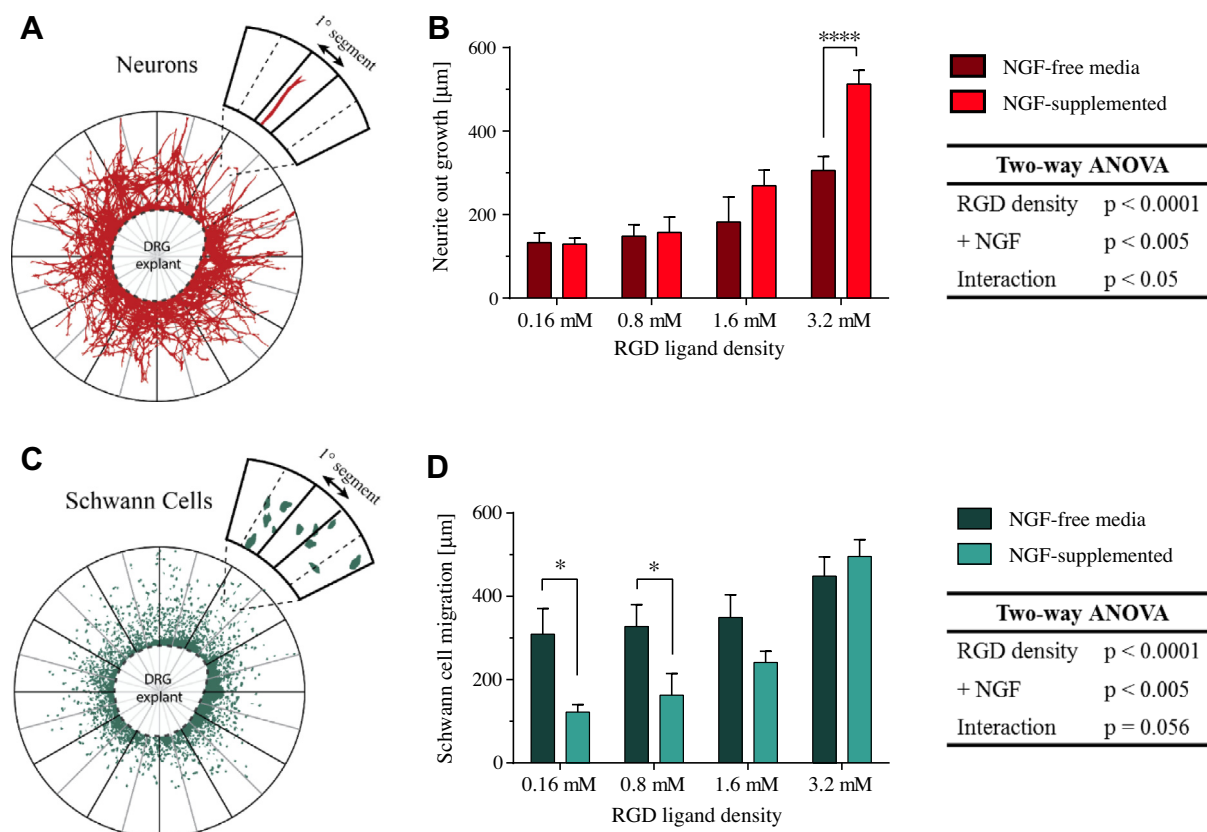


Fig. 2. Quantification of neurite outgrowth and Schwann cell migration distance. (A) Each DRG was divided into 1° segments. Neurite outgrowth in each segment was defined as the distance between the tip of the longest neurite and the explant boundary. (B) Neurite length increased synergistically with RGD ligand density and NGF supplementation. (C) Schwann cell migration was determined by the distance between the foremost migrating Schwann cell and the explant boundary in each 1° segment. (D) Schwann cell migration increased with RGD ligand density, while NGF supplementation limited the migration distance on low ligand density eECMs. Mean distances are depicted ± SEM. n = 6–13 DRGs per experimental condition. *p < 0.05 and ****p < 0.0001 for post-hoc *t*-tests with Bonferroni correction for multiple comparisons.

The statistical significance of gene regulation as a result of NGF supplementation was determined using log-transformed data ($n = 12$ DRGs) [42]. Because the \log_2 (fold change) approximated a normal distribution, a geometric mean of the fold change was found by averaging the log-transformed values and back-transforming to a natural scale. Similarly, the log-transformed data were used to calculate log-transformed confidence intervals, which were then converted into asymmetric confidence intervals on the natural scale. p -Values were calculated directly from log-transformed confidence intervals.

Co-localization of Schwann cells and neurites was determined, together with the number of migrating Schwann cells, by analyzing images of 3–13 DRGs for each of the eight eECM conditions. The effects of Schwann cell depletion, conditioned medium treatment and L1CAM blocking on neurite outgrowth were examined on 17–23 DRGs per sample and compared to outgrowth of their untreated counterparts using unpaired t -tests. As above, a sufficient number of DRGs were used to ensure that at least 1000 neurites and 1000 Schwann cells were analyzed for each condition.

3. Results and discussion

3.1. NGF synergistically enhances neurite outgrowth on RGD-presenting matrices

The effect of cell–matrix interactions on neurite outgrowth was evaluated by culturing DRGs on eECMs presenting one of four RGD ligand densities, with or without soluble NGF in the culture medium. Neurites were observed to extend on all four eECM formulations, regardless of NGF supplementation (Fig. 1B and C). However, outgrowth on 0.16 and 0.8 mM RGD eECMs was modest, consisting of a few delicate neurites 100–200 μm long. In matrices presenting higher RGD ligand densities, the number and length of outgrowing neurites increased dramatically. On the 3.2 mM RGD eECM, NGF-supplemented cultures produced a robust outgrowth of fine, hair-like neurite structures, while the NGF-free cultures exhibited more modest outgrowth and bundled neurites.

Both RGD ligand density and NGF supplementation were found to significantly increase neurite outgrowth ($p < 0.0001$ and $p < 0.005$, respectively, two-way ANOVA, Fig. 2A and B). Furthermore, a significant interaction term ($p < 0.05$) pointed to interplay between the RGD ligand density and NGF supplementation. In the highest ligand density eECM, medium supplementation with NGF increased the mean neurite outgrowth length by 68% ($p < 0.0001$, post-hoc t -test with Bonferroni correction), suggesting that these two parameters interacted synergistically to enhance outgrowth.

This RGD-dependent outgrowth is consistent with our previous reports for DRGs cultured within three-dimensional ELP eECMs, where addition of the RGD ligand significantly improved neurite outgrowth [25]. Previously, Sheppard et al. [43] also observed an increase in neurite outgrowth from DRGs in poly(ethylene glycol) gels as RGD concentration was increased from 0 to 5 mM. However, Schense and Hubbell [26] reported that neurite outgrowth was bimodally dependent on RGD ligand density at much lower ligand concentrations, with maximal outgrowth on fibrin matrices containing 18 μM and decreased outgrowth observed on matrices with higher RGD content (up to 87 μM). Neurite outgrowth in our microenvironments increased as the concentration of RGD ligands was increased from 0.16 to 3.20 mM (Supplemental Fig. S2A), which is consistent with the work of Sheppard et al. If we assume homogeneous spacing of RGD ligands in three dimensions, the approximate linear spacing between RGD ligands in the eECM ranges from 8.0 nm in the 3.2 mM RGD matrices to 22 nm in the 0.16 mM RGD matrices. Assuming that an integrin on the cell surface can penetrate approximately 18 nm into the

hydrogel [44], the 2-D density of RGD ligands accessible to cells varies from 3.5×10^4 ligands μm^{-2} in the 3.2 mM RGD matrices to 1.7×10^3 ligands μm^{-2} in the 0.16 mM matrices (see Supplemental information for the calculations). Previous studies investigating RGD ligand spacing on hydrogel substrates have demonstrated that varying the RGD spacing by a comparable factor resulted in significant changes in cell spreading and proliferation rate [45]. Consistent with previous reports [43,46], soluble plasma fibronectin (which contains the RGD ligand) from the FBS in the culture medium did not detrimentally affect cell adhesion and neurite extension on the engineered matrices.

3.2. NGF suppresses Schwann cell migration on low ligand density matrices

RGD ligand density and NGF supplementation were also found to be significant factors for Schwann cell migration distance (Fig. 2C and D). Similar to neurite outgrowth, the migration of Schwann cells increased with increasing RGD ligand density in the presence of NGF (Supplemental Fig. S2B). In contrast to neurite outgrowth, Schwann cell migration on the 3.2 mM RGD eECM was unaffected by supplementation with NGF. In fact, NGF had the greatest effect on Schwann cells migrating on the lower RGD ligand density eECMs, suppressing Schwann cell migration by as much as 61% on 0.16 mM RGD ($p < 0.05$, post-hoc t -test with Bonferroni correction).

A comparison between Schwann cell migration distance and the corresponding neurite outgrowth length in each condition indicated that enhanced cell–cell interactions may have been responsible for the slower migratory progress of Schwann cells in NGF-supplemented medium (Fig. 3A). In the absence of NGF, Schwann cell migration surpassed neurite outgrowth by an average of $167 \pm 8 \mu\text{m}$ (mean \pm SEM for all four eECM formulations without NGF, $n = 40$ DRGs). By contrast, Schwann cell migration in NGF-supplemented conditions tracked closely with neurite outgrowth, lagging by only $12 \pm 7 \mu\text{m}$ on average (mean \pm SEM for all four NGF-supplemented eECMs, $n = 33$ DRGs). Although NGF supplementation significantly altered the Schwann cell migration distance relative to neurite outgrowth ($p < 0.0001$ for each eECM formulation, t -test with Bonferroni correction), RGD ligand density did not have a significant effect (one-way ANOVAs). These results supported the hypothesis that the addition of NGF altered Schwann cell–neurite interactions, while RGD ligand density did not.

To verify that Schwann cell migration past neurites in NGF-free cultures was not attributable to a higher number of migratory Schwann cells, we compared the number of migrating cells in each of the eight conditions (Fig. 3B). Confirming the hypothesis, NGF supplementation was not a statistically significant predictor of the number of migrating Schwann cells. In contrast, increasing RGD ligand density significantly increased the number of migrating Schwann cells ($p < 0.0001$ for RGD ligand density, two-way ANOVA). These data agree with previous reports, which identified the presentation of RGD ligands as a regulator of neurite outgrowth and Schwann cell migration [22,47]. Therefore, the migration of Schwann cells past neurites in NGF-free cultures is not due to a higher number of migrating Schwann cells, suggesting that neurite–Schwann cell interactions may be modified by the presence of NGF.

3.3. Schwann cell–neurite contact is enhanced by NGF

Following an injury in the PNS, Schwann cells interact with neurons and encourage neurite extension by secreting neurotrophic factors, by synthesizing new ECM and by direct engagement with neurites through cell adhesion molecules [5]. Myelinating Schwann cells transition to a non-myelinating phenotype that is

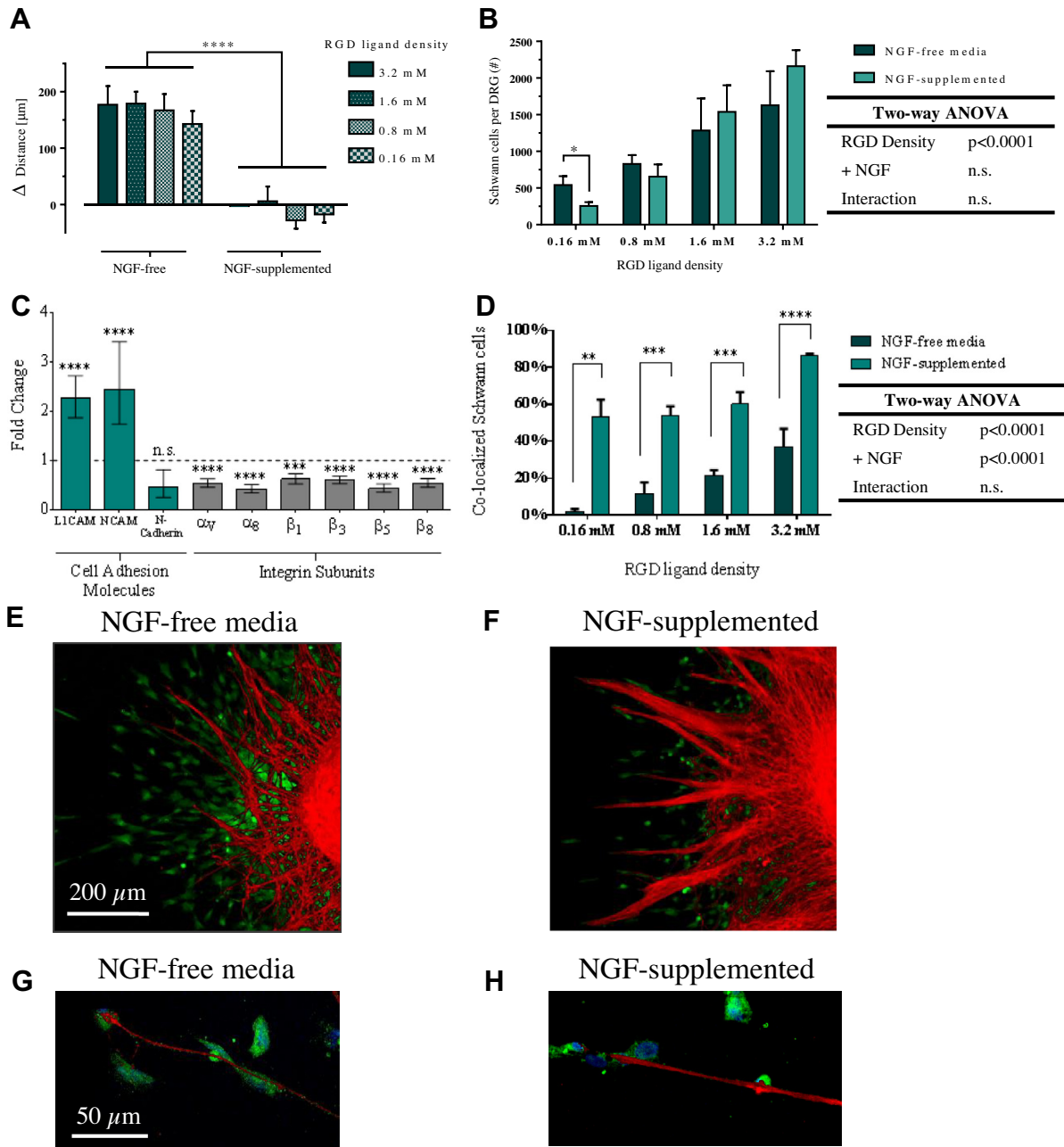


Fig. 3. Effect of NGF on coordinated outgrowth between neurites and Schwann cells. (A) Schwann cell migration distance past neurite outgrowth length (Δ Distance) was considerable in medium without NGF for all eECMs. The addition of NGF caused Schwann cell migration to track closely with neurite outgrowth. Mean \pm SEM, $n = 6$ –13 DRGs per condition. (B) The number of migrating Schwann cells increased with RGD ligand density, but not with NGF supplementation. Mean \pm SEM, $n = 3$ –16 DRGs per condition. (C) NGF supplementation resulted in a 2.3-fold up-regulation in mRNA encoding for L1CAM, as well as a down-regulation of integrin subunits. Geometric mean \pm asymmetric confidence interval (CI) ($\alpha = 0.05$) from log-transformed data, $n = 12$ DRGs. p -Values were calculated from log-transformed CI. (D) Co-localization of migrating Schwann cells with neurites increased with both RGD ligand density and NGF supplementation. Mean \pm SEM, $n = 3$ –13 DRGs per condition. (E–H) Overlay of β -III tubulin-positive neurites (red) on S100 protein-positive Schwann cells (green) with nuclei (blue), migrating on 3.2 mM RGD eECM (E and F) or 0.8 mM RGD eECM (G and H) in medium without (E and G) or with (F and H) NGF supplementation. * $p < 0.05$, ** $p < 0.01$, *** $p < 0.0005$, **** $p < 0.0001$ for post-hoc t -tests with Bonferroni correction for multiple comparisons.

characterized by increased expression of the cell adhesion molecules L1CAM, NCAM and N-cadherin [5]. L1CAM and NCAM facilitate contact between axonal growth cones and non-myelinating Schwann cells [48]. In particular, L1CAM has been shown to play a crucial role in nerve regeneration, as blocking antibodies directed against L1CAM inhibit neurite outgrowth in co-cultures with Schwann cells, whereas blocking antibodies against NCAM have been less effective [5]. As the regeneration process continues and Schwann cells begin to wrap around the extending neurites, the Schwann cells transition back to a myelinating phenotype, and

Schwann cell–neurite interactions become dominated by cell–cell adhesion through MAG [5,48].

Several groups have previously reported a link between NGF and the subsequent up-regulation of L1CAM [32,49]. Quantitative RT-PCR of DRGs in NGF-supplemented and NGF-free medium confirmed the up-regulation of mRNA encoding for L1CAM in the presence of NGF ($p < 0.0001$, Fig. 3C). This observation is consistent with previous studies demonstrating up-regulation of L1CAM in response to NGF binding by p75 [32]. Therefore, the exogenous addition of NGF to the culture medium may have enhanced

L1CAM engagement between Schwann cells and neurites during outgrowth. Quantitative RT-PCR also indicated an up-regulation of NCAM after treatment with NGF ($p < 0.0001$); however, previous studies have found that blocking NCAM-mediated interactions between neurites and Schwann cells did not significantly inhibit neurite outgrowth [5,10,50]. The post-translational modification of NCAM with polysialic acid (PSA) is known to regulate neurite outgrowth [51], and measuring the relative NCAM mRNA content via RT-PCR does not detect these modifications. Thus, the observed increase in expression of mRNA for NCAM may not correlate with increased production of NCAM-PSA previously implicated in neurite outgrowth. The expression of N-cadherin was not significantly affected by NGF treatment. In addition, NGF supplementation led to a slight overall decrease in mRNA encoding for RGD-binding integrin subunits known to be present in DRGs [52–55]. Together, these results imply that NGF had an overall effect of increasing cell–cell interactions via L1CAM, possibly at the expense of cell–matrix interactions.

We then used an image-based co-localization analysis to evaluate the hypothesis that NGF increases association between the outgrowing Schwann cells and neurites (Fig. 3D). The fraction of Schwann cells that were spatially distinct from the neuron-specific β -III tubulin stain was subtracted from unity to determine the fraction of migrating Schwann cells co-localized with neurites. Regardless of RGD ligand density, the addition of NGF to the culture medium resulted in a dramatic improvement in Schwann cell–neurite co-localization ($p < 0.01$ for 0.16 mM RGD, $p < 0.001$ for other eECMs, post-hoc t -test with Bonferroni correction). The increase in RGD ligand density from 0.16 to 3.20 mM also resulted in a corresponding increase in co-localization in both NGF-free and NGF-supplemented conditions (2–37% in the absence of NGF, 53–87% in NGF-supplemented medium). Representative images illustrate the co-localization of Schwann cells with neurites both on high ligand density eECMs (3.2 mM RGD, Fig. 3E and F) and low ligand density eECMs (0.8 mM RGD, Fig. 3G and H).

3.4. Neurite outgrowth requires L1CAM engagement in the presence of NGF

We hypothesized that Schwann cell–neurite contact is necessary for neurite outgrowth in NGF-supplemented cultures. To test this hypothesis, we depleted DRGs of Schwann cells without disrupting the overall explant architecture by including 7 μ M cytosine arabinoside (AraC) in the culture medium. AraC blocks DNA replication, thereby depleting the DRG structure of rapidly dividing cells and leaving a highly enriched neuronal population (Fig. 4A) [56]. Immunocytochemistry of these Schwann cell-depleted explants on eECMs confirmed the overwhelming absence of non-neuronal cells, although a small number of Schwann cells were observed (fewer than 10% of the migratory population in non-depleted explants).

Surprisingly, Schwann cell-depleted explants in the absence of exogenously added NGF exhibited a similar level of neurite outgrowth on the 3.2 mM RGD eECM as cultures without AraC (Fig. 4B and G). By contrast, Schwann cell-depleted explants cultured in NGF-supplemented medium were no longer able to extend robust, finely structured neurite outgrowths (Fig. 4B and H). Quantification of this outgrowth revealed a non-significant change in neurite outgrowth for NGF-free medium ($n = 23$ depleted explants, Fig. 4B) and an 84% decrease in neurite outgrowth attributable to Schwann cell depletion in NGF-supplemented medium ($p < 0.0001$, $n = 22$ depleted explants, Fig. 4B). These surprising results are contrary to the typically trophic effect of NGF supplementation in neural cultures.

In order to evaluate whether Schwann cell–neurite contact via L1CAM in particular was responsible for neurite outgrowth in

NGF supplemented medium, we added a monoclonal antibody directed against the L1-like antigen 8D9 to the culture medium. The 8D9 antigen is the avian ortholog to L1CAM in mammals, and an antibody against this antigen is known to block L1CAM-mediated signaling [57,58]. We hypothesized that the level of Schwann cell–neurite interactions would be dramatically reduced due to blocking of L1CAM by the 8D9 antibody. Neurites in NGF-free medium exhibited similar outgrowth on the 3.2 mM RGD eECM, both with and without 8D9 treatment ($n = 22$ explants, Fig. 4B and C). In contrast, neurite lengths in the NGF-supplemented, L1CAM-blocked conditions were reduced by 48% as compared to their counterparts without the blocking treatment ($p < 0.0001$, $n = 21$ explants, Fig. 4B and D). Therefore, neurite outgrowth in the presence of exogenous NGF appears to require L1CAM-mediated Schwann cell–neurite contact, while this interaction is not required in the absence of NGF. Furthermore, the L1CAM blocking and Schwann cell depletion data suggest that neurite outgrowth in the absence of NGF is primarily mediated by the RGD ligand presented by the eECM. This is consistent with RT-PCR data indicating higher expression of RGD-binding integrins in NGF-free cultures (Fig. 3C).

While L1CAM blocking significantly reduced neurite outgrowth in NGF-treated cultures, neurite outgrowth in the L1CAM-blocked cultures was still greater than in the Schwann cell-depleted cultures. In addition to the possibility of incomplete L1CAM blocking by the 8D9 antibody, soluble factors secreted by the Schwann cells or other mechanisms of Schwann cell–neurite contact may be responsible for this increased outgrowth [5]. To evaluate the effects of Schwann cell secreted factors, Schwann cell-depleted explants were treated with conditioned medium from cultures of intact DRG explants, with or without exogenous NGF. Schwann cell-depleted cultures treated with both conditioned medium and NGF exhibited significantly decreased neurite outgrowth relative to NGF-treated co-cultures ($p < 0.0001$, $n = 17$ explants, Fig. 4B and F) and similar levels of outgrowth when compared to L1CAM-blocked cultures. The addition of conditioned medium to the Schwann cell-depleted, NGF-treated cultures increased neurite outgrowth relative to Schwann cell-depleted cultures without conditioned medium ($p < 0.05$), indicating that soluble factors secreted by Schwann cells may permit partial recovery of neurite outgrowth. This relative increase in outgrowth provides a potential explanation for the increased outgrowth observed in L1CAM-blocked cultures relative to Schwann cell-depleted cultures that have been treated with NGF. Interestingly, in the absence of exogenous NGF, the addition of conditioned medium to Schwann cell-depleted cultures results in decreased neurite outgrowth relative to Schwann cell-depleted cultures treated with standard culture medium ($p < 0.01$, $n = 17$ explants, Fig. 4B and E). Schwann cells are known to secrete neurotrophins, including NGF, following an injury in the PNS [5]. Thus, the conditioned medium from DRG cultures containing Schwann cells likely contains NGF, which would lead to decreased neurite outgrowth, as demonstrated in the cultures treated with exogenous NGF.

In addition to Schwann cell–secreted soluble factors, direct Schwann cell–neurite engagement via N-cadherin is also known to play a role in Schwann cell-mediated neurite outgrowth [5,59]. In particular, cell–cell contact via N-cadherin may explain the observation that migrating Schwann cells largely remain co-localized with extending neurites in the presence of L1CAM blocking (Supplemental Fig. S3). NGF treatment had no significant effect on N-cadherin expression (Fig. 3C), suggesting that N-cadherin-mediated Schwann cell–neurite contact is not responsible for the differences in outgrowth observed between NGF treated and untreated cultures. Future studies will investigate the role of N-cadherin-mediated Schwann cell–neurite interactions by disrupting N-cadherin binding using a function blocking antibody, similar

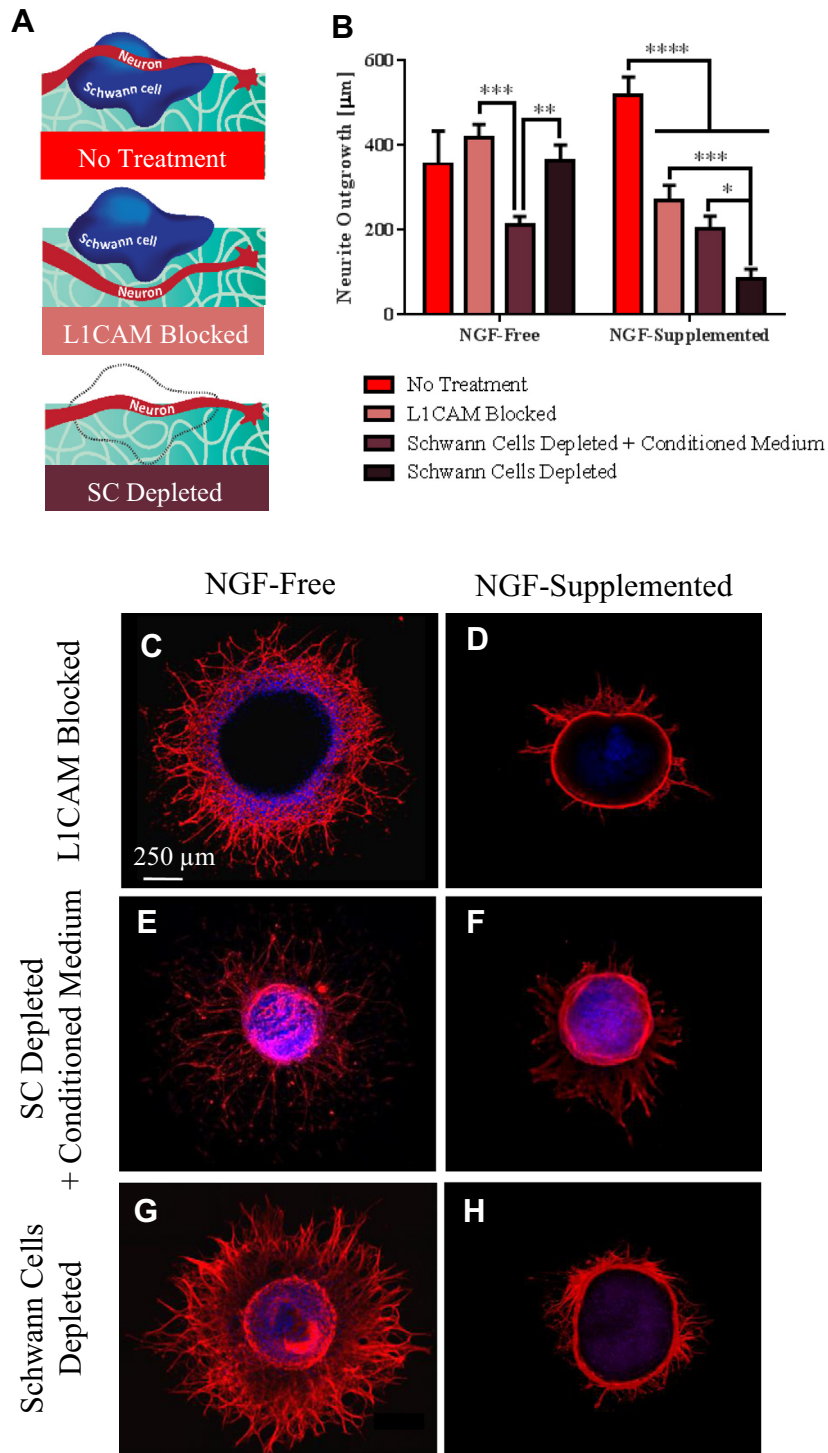


Fig. 4. Neurite outgrowth on 3.2 mM RGD-ELP, with and without NGF supplementation, in L1CAM-blocking culture as well as Schwann cell-depleted explants. (A) Schematic depicting L1CAM blocking and Schwann cell-depleted conditions. (B) Quantification of neurite outgrowth on 3.2 mM RGD eECMs with and without NGF supplementation, in culture medium without global treatment (No treatment), with the L1CAM-blocking 8D9 antibody (L1CAM blocked) or the addition of proliferation-interfering cytosine arabinoside (Schwann cells depleted), in the presence or absence of Schwann cell-conditioned medium. L1CAM blocking and Schwann cell depletion significantly reduced the ability of neurites to grow in the presence of NGF. Mean \pm SEM; * $p < 0.05$, ** $p < 0.01$, *** $p < 0.001$ and **** $p < 0.0001$. (C–H) Representative images of red neurites (β -III tubulin) overlaid on blue nuclei (DAPI). (C) DRG in NGF-free medium with L1CAM-blocking 8D9 antibody; (D) DRG in NGF-supplemented medium with L1CAM-blocking 8D9 antibody; (E) Schwann cell-depleted DRG cultured with conditioned medium in the absence of NGF; (F) Schwann cell-depleted DRG cultured with conditioned medium in the presence of NGF; (G) Schwann cell-depleted DRG in NGF-free medium; (H) Schwann cell-depleted DRG in NGF-supplemented medium.

to the strategy employed for L1CAM in the present study, or using a function blocking peptide [59].

The dependence of neurite outgrowth on contact with Schwann cells when cultured on RGD-presenting matrices in the presence of

NGF is a surprising result, given that previous studies have demonstrated integrin-dependent neurite outgrowth in neuronal cultures supplemented with NGF. We have previously reported enhanced neurite outgrowth from neuronal-like PC12 cells on eECM gels

[27]. Muller et al. cultured sensory neurons derived from chick DRGs on adsorbed fibronectin, which contains a similar RGD ligand to that presented by our eECM, and found that RGD engagement by the $\alpha_8\beta_1$ integrin pair facilitated neurite extension [55]. In the present study, qRT-PCR revealed a decrease in expression of both α_8 and β_1 integrin subunits upon treatment with NGF (Fig. 3C), providing a possible mechanism by which outgrowth on RGD matrices can be decreased by NGF treatment. Other studies have investigated the role of the laminin-binding $\alpha_1\beta_1$ integrin pair on neurite outgrowth in rat DRG sensory neurons [60], PC12 cells and rat hippocampal neurons [61]. Both studies used cyclic RGD peptides to block substrate engagement by the β_1 integrin subunit. Rankin et al. [61] reported enhanced neurite outgrowth on laminin-coated substrates upon treatment with NGF. Our qRT-PCR results indicate a down-regulation of RGD-binding integrin subunits, including β_1 , upon treatment with NGF (Fig. 3C). However, it is possible that NGF treatment results in the up-regulation of other integrins, such as the previously investigated α_1 subunit, that would permit outgrowth on matrices presenting other adhesion ligands.

The data presented in this paper demonstrate that L1CAM interactions mediate the synergistic enhancement of neurite outgrowth on RGD-presenting eECMs in NGF-supplemented medium. While NGF is generally thought of as neurotrophic, our data clearly show that its activity is context dependent; in the absence of Schwann cells, NGF can suppress neurite outgrowth (Fig. 4B, G and H). Furthermore, we demonstrate that the neurotrophic activity of NGF depends critically on RGD ligand density in these microenvironments; significant enhancement of neurite outgrowth by NGF was only observed on the highest RGD ligand density matrix tested (Figs. 1B and C and 2B). In contrast, NGF supplementation caused Schwann cell migration to track closely with neurite length across the full range of RGD ligand density eECMs (Fig. 3A). Therefore, in these particular microenvironments the predominant function of NGF appeared to be the enhancement of interactions between extending neurites and migrating Schwann cells (Fig. 3D–F). These cell–cell interactions were dependent on L1CAM binding (Fig. 4B–D) and were required for synergistically enhanced neurite outgrowth in response to RGD ligands and NGF. These results have potential implications for the design of nerve guides for PNS regeneration.

4. Conclusions

We have engineered a microenvironment capable of regulating the cell–matrix and cell–cell interactions among neurites and Schwann cells extending from chick dorsal root ganglia. While the incorporation of integrin-binding RGD ligands and supplementation with NGF individually contributed to neurite outgrowth, these two strategies combined synergistically to produce significantly enhanced outgrowth. Additionally, neurites in NGF-supplemented medium extended on the eECM via a Schwann cell-mediated, L1CAM-dependent mechanism. As a result, neurites in NGF-supplemented medium were unable to extend into the surrounding matrix without the assistance of Schwann cells. Our results highlight the synergistic effect of cell–matrix and cell–cell interactions in neural outgrowth behavior and support the further development of regenerative therapies for peripheral nerve injury that integrate cues to simultaneously control cell–matrix and cell–cell engagement.

Acknowledgements

N.H.R. acknowledges support from a Stanford Graduate Fellowship and a National Science Foundation Graduate Fellowship. The authors acknowledge funding from the National Institutes of

Health (1DP2-OD006477, R01-DK085720, R21-AR062359-01) and the National Science Foundation (DMR-0846363). The authors thank Ruby E. Dewi (Stanford University) for assistance with PCR experiments and Kyle Lampe (University of Virginia) for DRG culture training, as well as Ranjan Kumar, Jeff Biernaskie and Rajiv Midha (University of Calgary) for providing a protocol for the depletion of Schwann cells from DRGs.

Appendix A. Figures with essential colour discrimination

Certain figures in this article, particularly Figures 1–4, are difficult to interpret in black and white. The full colour images can be found in the on-line version, at <http://dx.doi.org/10.1016/j.actbio.2014.10.008>.

Appendix B. Supplementary data

Supplementary data associated with this article can be found in the online version, at <http://dx.doi.org/10.1016/j.actbio.2014.10.008>.

References

- [1] Dubový P. Wallerian degeneration and peripheral nerve conditions for both axonal regeneration and neuropathic pain induction. *Ann Anat* 2011;193:267–75.
- [2] Scheib J, Hoke A. Advances in peripheral nerve regeneration. *Nat Rev Neurol* 2013;9:668–76.
- [3] Brown MC, Perry V, Lunn E, Gordon S. Macrophage dependence of peripheral sensory nerve regeneration: possible involvement of nerve growth factor. *Neuron* 1991;6:359–70.
- [4] Son Y-J, Thompson WJ. Schwann cell processes guide regeneration of peripheral axons. *Neuron* 1995;14:125–32.
- [5] Fu SY, Gordon T. The cellular and molecular basis of peripheral nerve regeneration. *Mol Neurobiol* 1997;14:67–116.
- [6] Ide C, Tohyama K, Yokota R, Nitatori T, Onodera S. Schwann cell basal lamina and nerve regeneration. *Brain Res* 1983;288:61–75.
- [7] Eldridge CF, Bunge MB, Bunge RP. Differentiation of axon-related Schwann cells in vitro: II. Control of myelin formation by basal lamina. *J Neurosci* 1989;9:625–38.
- [8] Chan JR, Jolicœur C, Yamauchi J, Elliott J, Fawcett JP, Ng BK, et al. The polarity protein Par-3 directly interacts with p75NTR to regulate myelination. *Science* 2006;314:832–6.
- [9] Nave K-A. Myelination and support of axonal integrity by glia. *Nature* 2010;468:244–52.
- [10] Bixby J, Lilien J, Reichardt L. Identification of the major proteins that promote neuronal process outgrowth on Schwann cells in vitro. *J Cell Biol* 1988;107:353–61.
- [11] Martini R, Xin Y, Schachner M. Restricted localization of L1 and N-CAM at sites of contact between Schwann cells and neurites in culture. *Glia* 1994;10:70–4.
- [12] Court FA, Wrabetz L, Feltri ML. Basal lamina: Schwann cells wrap to the rhythm of space–time. *Curr Opin Neurobiol* 2006;16:501–7.
- [13] Chernousov MA, Yu WM, Chen ZL, Carey DJ, Strickland S. Regulation of Schwann cell function by the extracellular matrix. *Glia* 2008;56:1498–507.
- [14] Milner R, Wilby M, Nishimura S, Boylen K, Edwards G, Fawcett J, et al. Division of labor of Schwann cell integrins during migration on peripheral nerve extracellular matrix ligands. *Dev Biol* 1997;185:215–28.
- [15] Martini R. Expression and functional roles of neural cell-surface molecules and extracellular-matrix components during development and regeneration of peripheral nerves. *J Neurocytol* 1994;23:1–28.
- [16] Hersel U, Dahmen C, Kessler H. RGD modified polymers: biomaterials for stimulated cell adhesion and beyond. *Biomaterials* 2003;24:4385–415.
- [17] Ruoslahti E, Pierschbacher MD. New perspectives in cell adhesion: RGD and integrins. *Science* 1987;238:491–7.
- [18] Baron-van Evercooren A, Kleinman H, Ohno S, Marangos P, Schwartz JP, Dubois-Dalq M. Nerve growth factor, laminin, and fibronectin promote neurite growth in human fetal sensory ganglia cultures. *J Neurosci Res* 1982;8:179–93.
- [19] Bozkurt A, Brook G, Moellers S, Lassner F, Sellhaus B, Weis J, et al. Assessment of axonal growth using dorsal root ganglia explants in a novel three-dimensional collagen matrix. *Tissue Eng* 2007;13:2971–9.
- [20] Lemmon V, Burden SM, Payne HR. Neurite growth on different substrates: permissive versus instructive influences and the role of adhesive strength. *J Neurosci* 1992;12:818–26.
- [21] Pittier R, Sauthier F, Hubbell JA, Hall H. Neurite extension and in vitro myelination within three-dimensional modified fibrin matrices. *J Neurobiol* 2005;63:1–14.
- [22] Zhang Z, Yoo R, Wells M, Beebe Jr TP, Biran R, Tresco P. Neurite outgrowth on well-characterized surfaces: preparation and characterization of chemically

- and spatially controlled fibronectin and RGD substrates with good bioactivity. *Biomaterials* 2005;26:47–61.
- [23] Bockelmann J, Klinkhammer K, von Holst A, Seiler N, Faissner A, Brook GA, et al. Functionalization of electrospun poly (ϵ -caprolactone) fibers with the extracellular matrix-derived peptide GRGDS improves guidance of Schwann cell migration and axonal growth. *Tissue Eng Part A* 2011;17:475–86.
- [24] Holmes TC, de Lacalle S, Su X, Liu G, Rich A, Zhang S. Extensive neurite outgrowth and active synapse formation on self-assembling peptide scaffolds. *Proc Natl Acad Sci* 2000;97:6728–33.
- [25] Lampe KJ, Antaris AL, Heilshorn SC. Design of three-dimensional engineered protein hydrogels for tailored control of neurite growth. *Acta Biomater* 2013;9:5590–9.
- [26] Schense JC, Hubbell J. Three-dimensional migration of neurites is mediated by adhesion site density and affinity. *J Biol Chem* 2000;275:6813–8.
- [27] Straley KS, Heilshorn SC. Independent tuning of multiple biomaterial properties using protein engineering. *Soft Matter* 2009;5:114–24.
- [28] Hari A, Djohar B, Skutella T, Montazeri S. Neurotrophins and extracellular matrix molecules modulate sensory axon outgrowth. *Int J Dev Neurosci* 2004;22:113–7.
- [29] Gallo G, Lefcort FB, Letourneau PC. The trkA receptor mediates growth cone turning toward a localized source of nerve growth factor. *J Neurosci* 1997;17:5445–54.
- [30] Herrup K, Shooter EM. Properties of the β nerve growth factor receptor of avian dorsal root ganglia. *Proc Natl Acad Sci* 1973;70:3884–8.
- [31] Kaplan DR, Hempstead BL, Martin-Zanca D, Chao MV, Parada LF. The trk proto-oncogene product: a signal transducing receptor for nerve growth factor. *Science* 1991;252:554–8.
- [32] Itoh K, Brackenbury R, Akeson RA. Induction of L1 mRNA in PC12 cells by NGF is modulated by cell–cell contact and does not require the high-affinity NGF receptor. *J Neurosci* 1995;15:2504–12.
- [33] Wood PM, Schachner M. Inhibition of Schwann cell myelination in vitro by antibody to the L1 adhesion molecule. *J Neurosci* 1990;10:3635–45.
- [34] Schafer MK, Frotscher M. Role of L1CAM for axon sprouting and branching. *Cell Tissue Res* 2012;349:39–48.
- [35] Gast D, Riedle S, Kiefel H, Mürköster SS. The RGD integrin binding site in human L1-CAM is important for nuclear signaling. *Exp Cell Res* 2008;314:2411–8.
- [36] Voura EB, Ramjeesingh RA. Involvement of integrin $\alpha\beta3$ and cell adhesion molecule L1 in transendothelial migration of melanoma cells. *Mol Biol Cell* 2001;12:2699–710.
- [37] Thelen K, Kedar V, Panicker AK, Schmid R-S, Midkiff BR, Maness PF. The neural cell adhesion molecule L1 Potentiates integrin-dependent cell migration to extracellular matrix proteins. *J Neurosci* 2002;22:4918–31.
- [38] Heilshorn SC, DiZio KA, Welsh ER, Tirrell DA. Endothelial cell adhesion to the fibronectin CS5 domain in artificial extracellular matrix proteins. *Biomaterials* 2003;24:4245–52.
- [39] He Y, Baas PW. Growing and working with peripheral neurons. In: Wilson L, Matsudaira P, editors. *Methods in cell biology*. Academic Press; 2003. p. 17–35.
- [40] Hurlbert SH. Pseudoreplication and the design of ecological field experiments. *Ecol Monogr* 1984;54:187–211.
- [41] Schwarz CJ. Estimating an overall mean with subsampling. In: *Sampling, regression, experimental design and analysis for environmental scientists, biologists, and resource managers*. British Columbia: Simon Fraser University; 2013. p. 484.
- [42] Bland JM, Altman DG. Statistics notes: transformations, means, and confidence intervals. *BMJ* 1996;312:1079.
- [43] Shepard JA, Stevans AC, Holland S, Wang CE, Shikanov A, Shea LD. Hydrogel design for supporting neurite outgrowth and promoting gene delivery to maximize neurite extension. *Biotechnol Bioeng* 2012;109:830–9.
- [44] Xiong J-P, Stehle T, Diefenbach B, Zhang R, Dunker R, Scott DL, et al. Crystal structure of the extracellular segment of integrin $\alpha V\beta3$. *Science* 2001;294:339–45.
- [45] Lee KY, Alsberg E, Hsiong SX, Comisar WA, Linderman JJ, Ziff R, et al. Nanoscale adhesion ligand organization regulates osteoblast proliferation and differentiation. *Nano Lett* 2004;4:1501–6.
- [46] Gunn JW, Turner SD, Mann BK. Adhesive and mechanical properties of hydrogels influence neurite extension. *J Biomed Mater Res* 2005;72A:91–7.
- [47] Akassoglou K, Akpınar P, Murray S, Strickland S. Fibrin is a regulator of Schwann cell migration after sciatic nerve injury in mice. *Neurosci Lett* 2003;338:185–8.
- [48] Martini R, Schachner M. Immunoelectron microscopic localization of neural cell adhesion molecules (L1, N-CAM, and myelin-associated glycoprotein) in regenerating adult mouse sciatic nerve. *J Cell Biol* 1988;106:1735–46.
- [49] Bock E, Richter-Landsberg C, Faissner A, Schachner M. Demonstration of immunochemical identity between the nerve growth factor-inducible large external (NILE) glycoprotein and the cell adhesion molecule L1. *EMBO* 1985;4:2765–8.
- [50] Seilheimer B, Schachner M. Studies of adhesion molecules mediating interactions between cells of peripheral nervous system indicate a major role for L1 in mediating sensory neuron growth on Schwann cells in culture. *J Cell Biol* 1988;107:341–51.
- [51] Doherty P, Cohen J, Walsh FS. Neurite outgrowth in response to transfected N-CAM changes during development and is modulated by polysialic acid. *Neuron* 1990;5:209–19.
- [52] Tomaselli KJ, Doherty P, Emmett CJ, Damsky CH, Walsh FS, Reichardt LF. Expression of beta 1 integrins in sensory neurons of the dorsal root ganglion and their functions in neurite outgrowth on two laminin isoforms. *J Neurosci* 1993;13:4880–8.
- [53] Condic M, Letourneau P, Condic P. Ligand-induced changes in integrin expression regulate neuronal adhesion and neurite outgrowth. *Nature* 1997;389:852–6.
- [54] Yip PM, Zhao X, Montgomery AM, Siu CH. The Arg–Gly–Asp motif in the cell adhesion molecule L1 promotes neurite outgrowth via interaction with the $\alpha V\beta3$ integrin. *Mol Biol Cell* 1998;9:277–90.
- [55] Muller U, Bossy B, Venstrom K, Reichardt LF. Integrin $\alpha8\beta1$ promotes attachment, cell spreading, and neurite outgrowth on fibronectin. *Mol Biol Cell* 1995;6:433–48.
- [56] Wood PM. Separation of functional Schwann cells and neurons from normal peripheral nerve tissue. *Brain Res* 1976;115:361–75.
- [57] Lagenaur C, Lemmon V. An L1-like molecule, the 8D9 antigen, is a potent substrate for neurite extension. *Proc Natl Acad Sci USA* 1987;84:7753–7.
- [58] Lemmon V, McLoon SC. The appearance of an L1-like molecule in the chick primary visual pathway. *J Neurosci* 1986;6:2987–94.
- [59] Wanner IB, Wood PM. N-Cadherin mediates axon-aligned process growth and cell–cell interaction in rat Schwann cells. *J Neurosci* 2002;22:4066–79.
- [60] Tucker BA, Rahimtula M, Mearow KM. Integrin activation and neurotrophin signaling cooperate to enhance neurite outgrowth in sensory neurons. *J Comp Neurol* 2005;486:267–80.
- [61] Rankin SL, Guy CS, Mearow KM. Neurite outgrowth is enhanced by laminin-mediated down-regulation of the low affinity neurotrophin receptor, p75NTR. *J Neurochem* 2008;107:799–813.